Increased Sensitivity of Loss of Field Protection based on Admittance Measurement

Hans-Joachim Herrmann, Siemens AG, E D EA PRO LM1, Nürnberg
Andre Smit, Siemens Energy, Wendell NC

This contribution focuses on loss of field protection and introduces the admittance measuring technique. The theoretical background is covered extensively to facilitate a clear description of the factors associated with loss of field (under-excitation). Apart from deriving the stability limits, the transformation is described of the capability diagram to the admittance plane and consequently the admittance and impedance measuring techniques are compared. After introducing the „Admittance measuring technique" and typical protection characteristics some practical applications are described. These are primarily focused on the different methods for deriving the setting values. The simplicity of converting impedance setting values of existing relays to admittance settings is also illustrated. Setting and test recommendations are given. With examples from transient tests with a RTDS system and real loss of field faults the transient behavior and the reaction of the protection is demonstrated.

Keywords:
Generator protection, numerical protection, loss of field, under-excitation, static stability, impedance measurement, admittance measurement

1. Introduction

Under-excitation of a generator or a total loss of excitation can result from a short circuit or open circuit in the excitation circuit, a mal-operation of the automatic voltage regulator, incorrect control of generators and transformers, or in the event of a generator connected to a system with excessive capacitive load. In this context under-excitation means that the excitation of the synchronous machine is less than required for stable operation at a particular power level. This excitation limit determines the steady state stability characteristic of the generator. If the excitation is not sufficient to provide the power demanded of the generator, then this stability limit is exceeded. The machine will slip and thereby obtain the required excitation from the connected three phase system.
Depending on the construction of the generator, nature of the excitation circuit, system conditions, the amount of supplied power as well as the influence of voltage and power regulators (AGC), rotor acceleration may result in local overheating in rotor and stator, over-voltages on the rotor, mechanical impact on the generator mountings and power swings in the three phase system. In addition the large reactive power consumption can trigger an wide area voltage collapse. To prevent, or at least limit the duration of these harmful effects loss of field protection (Siemens call it under-excitation protection) is required to detect this under-excited condition, and initiate timely disconnection of the machine.

The protection function may be implemented in different ways. The impedance measurement [1, 2], is a widely applied measurement principle. Amongst other reasons this technique was chosen due to the widespread and proven use of impedance measuring elements in electro-mechanical relays. Approximately 40 years ago, Siemens however adopted a different route [3, 4]. A solution was found, which on the one hand may be directly derived from the capability diagram of the generator and on the other hand was immune to fluctuations of the generator voltage. This required a transformation of the generator diagram to the admittance plane and the processing of admittance measured values.

2. The Capability Diagram of Generators

To aid the following dissertation, the definition of the fundamental electrical quantities is provided hereunder:

- **Sign convention**: exported power (P, Q >0) is positive (generator reference arrow-system is used)
- **Apparent power**: described by the symbol **S** and has the dimension **VA** (kVA, MVA)
- **Active power:** described by the symbol **P** and the dimension **W** (kW, MW)
- **Reactive power:** described by the symbol **Q** and the dimension **Var** (kVar, MVar)
- When **per unit** (p.u.) values are used, the generator nominal values such as the nominal apparent power S_N, nominal voltage V_N, and nominal current I_N are used for the conversion.

According to the Cartesian co-ordinate system definition (x-axis = real component and y-axis = imaginary component), the first quadrant defines the operating range (P > 0 and Q > 0) of the generator. In the event of under-excitation (loss of field), operation is in the 4th quadrant (P > 0 and Q < 0). Graphic representation of the los of field protection takes place in the 4th quadrant. To avoid "neck strain", the diagram is often rotated to the left and mirrored in text books (refer to figure1). The author adopts this form of representation.

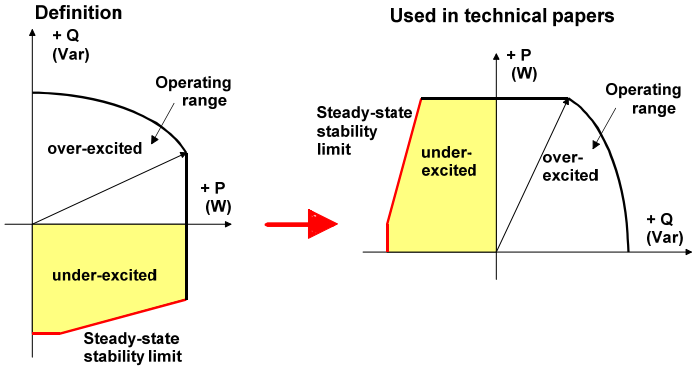

Figure 1: Alternative representation of the capability diagram

The stability limit is derived from the equations for the active and reactive power of the machine [5, 6]. It is assumed that the generator operates on an infinite network. The terminal voltage of generator is equal the network voltage. Equation (1) and equation (2) are the general defining equations and may be used directly for the salient pole generator, which has different direct axis and quadrature axis reactance. Due to the difference in x_d and x_q a reluctance response circle with the diameter ($V^2 \frac{x_d - x_q}{x_d\, x_q}$) results. This circle indicates the steady state power that the generator can produce with zero excitation (E = 0).

$$P = 3\frac{E\,V}{x_d}\sin\vartheta + 3\frac{V^2}{2}\frac{x_d - x_q}{x_d\, x_q}\sin 2\vartheta \qquad (1)$$

$$Q = 3\frac{E\,V}{x_d}\cos\vartheta - 3\frac{V^2}{x_d}\left(1 + \frac{x_d - x_q}{x_q}\sin^2\vartheta\right) \qquad (2)$$

with:

	E	rotor voltage (field e.m.f.) as a phase to star point voltage in p.u.
	V	terminal voltage (a phase to star point voltage) of the generator in p.u.
	x_d	synchronous direct axis reactance in p.u.
	x_q	synchronous quadrature axis reactance in p.u.
	ϑ	rotor angle (angular displacement)

Note: *If the phase-to-phase voltage representation is used in equation (1) to (4) the factor 3 must be removed.*

In the case of turbo generators the equations (1), (2) are simplified as the direct axis (x_d) and quadrature axis (x_q) reactance are approximately the same.

$$P = 3\frac{E\,V}{x_d}\sin\vartheta \qquad (3)$$

$$Q = 3\frac{E\,V}{x_d}\cos\vartheta - 3\frac{V^2}{x_d} \qquad (4)$$

In the case of an ideal turbo generator, the theoretical stability limit is $\vartheta = 90°$. Accordingly the limit value in the derived representation is given by the direct axis reactance x_d. For the salient pole generator, this limit is dependent on the reactance's x_d and x_q, as well as excitation and the terminal voltage. The base point on theoretical limit on the Q-axis is determined by the quadrature axis reactance x_q. The permitted rotor angle ϑ (theoretical stability limit) is less than 90°. These limits are graphically shown in figure 2 and 3 by means of the voltage and current vectors, as well as the capability diagram for both machine types.

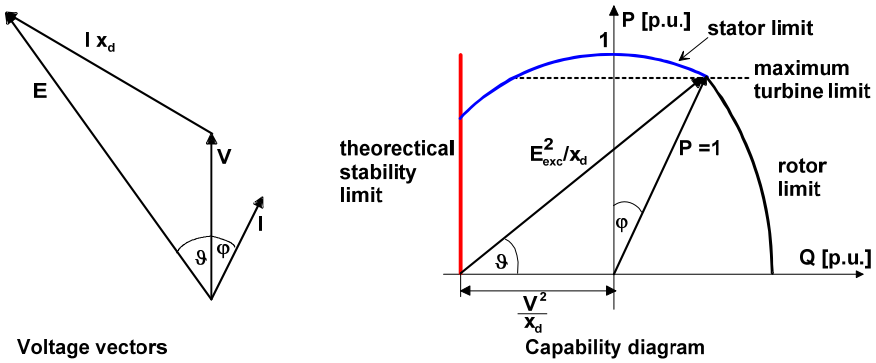

Figure 2: Vector and capability diagram of the turbo generator with $x_d = x_q$ (E_{exc} excitation voltage; I stator current)

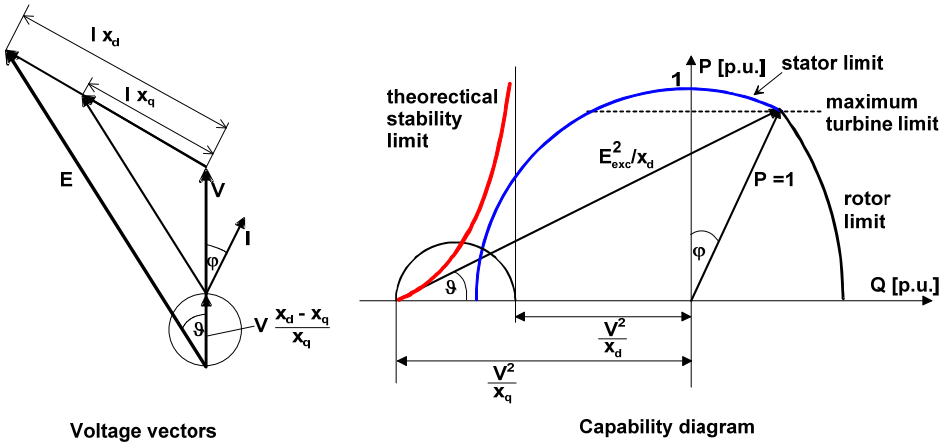

Figure 3: Vector and capability diagram of the salient pole generator ($x_d \neq x_q$)

From these diagrams it is apparent that the operating range of the generator is limited:

In the *over-excited range*:
by the power supplied by the turbine and the excitation (rotor values)
and
in the *under-excited range:*
by the power supplied by the turbine, the stator limits or the stability limit.

For operation on an interconnected system, the actual (practical) stability limits apply. These take into consideration the superseding reactances (e.g. unit transformer) which are always present, and a security margin (approximately 10% reserve at changing load). The actual admissible value for stability is therefore smaller than the theoretical value. The manufacturer of the generator specifies the limits that must be adhered to with the capability diagram. As in figure 1, various representations and scales of the axes can be found. These may have dimensions (MW, Mvar) or be dimensionless or per unit values (p.u.). The latter representation is preferred. If the values in a dimensioned characteristic are divided by the nominal apparent power, the result is the p.u. representation.
,

The following figures 4 and 5 provide an example of a turbo generator and salient pole generator capability diagram.

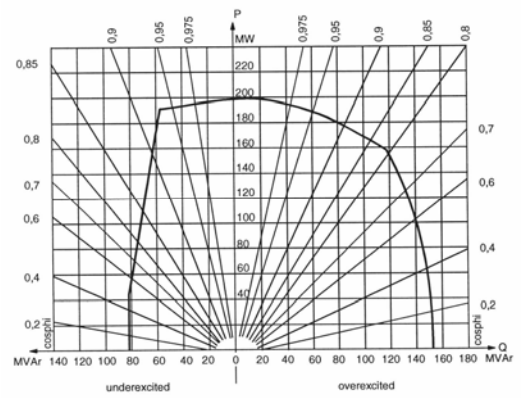

Figure 4: Capability diagram of a turbo generator

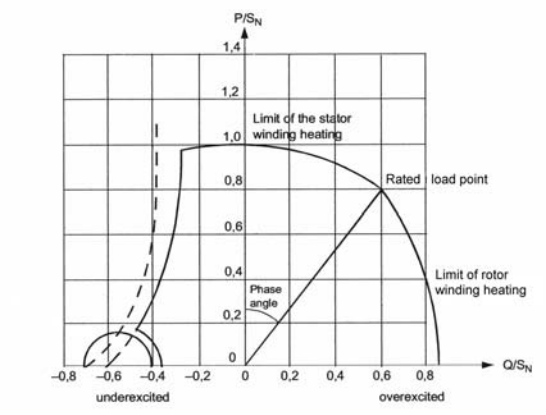

Figure 5: capability diagram of a salient pole generator

In the case of the turbo generator the stability curve is shifted to the right due to the superseding reactances, when compared to the theoretical curve. On the other hand, in the case of the salient pole generator, the theoretical stability characteristic is shifted to the right as a whole. The intersection with the reactive power axis is approximately at the centre of the reluctance power circle, as the theoretical intersection ($-V^2/x_q$) is instable as a result of the missing directional force [5].

The representation in the capability diagram is applicable with nominal voltage and current (V_N, I_N). Constant voltage may however not always be assumed. The following computation example illustrates the influence on the stability limits by variation of the voltage. The theoretical stability limit of the turbo generator (refer to figure 2) is used to illustrate the influence of a 10% change in the voltage [7].

If the excitation is equal to 0 the rotor voltage E=0. The maximum reactive power that can be imported is $Q = -V^2/x_d$, and reaches the following values:

$$\text{At}: V = 0.9: \; Q = -\frac{V^2}{x_d} = -\frac{0{,}9^2}{x_d} = -\frac{0.81}{x_d}$$

$$\text{At}: V = 1.1: \; Q = -\frac{V^2}{x_d} = -\frac{1{,}1^2}{x_d} = -\frac{1.21}{x_d}$$

Compared to the value at nominal voltage, the stability limit is shifted to the right during under-voltage conditions and further limits the amount of reactive power that may be imported. The influence is proportional to the square of the voltage. The over-voltage conditions are not critical as the stability limit is shifted to the left in this case.

The foregoing explanations apply to slow variations of system conditions. During sudden changes of load or system conditions, transient quantities apply, and a transient response will occur. Therefore a dynamic stability limit also exists. To reach a simplified approximation, the transient values (x'_d, x'_q and E‘) are applied to equation (1) and (2) [5]. In figure 6 the basic result is shown. For this purpose it was assumed that the steady state and transient quadrature axis reactance is the same. From the diagram it is apparent that the machine may even remain stable in the “dynamic” condition with a rotor angle >90°. An analogy with the turbo generator can also be found. In this case the dynamic stability limit is determined by the transient direct axis reactance. In practice the limit is also greater than 90° and is in the range between 110 and 120°.

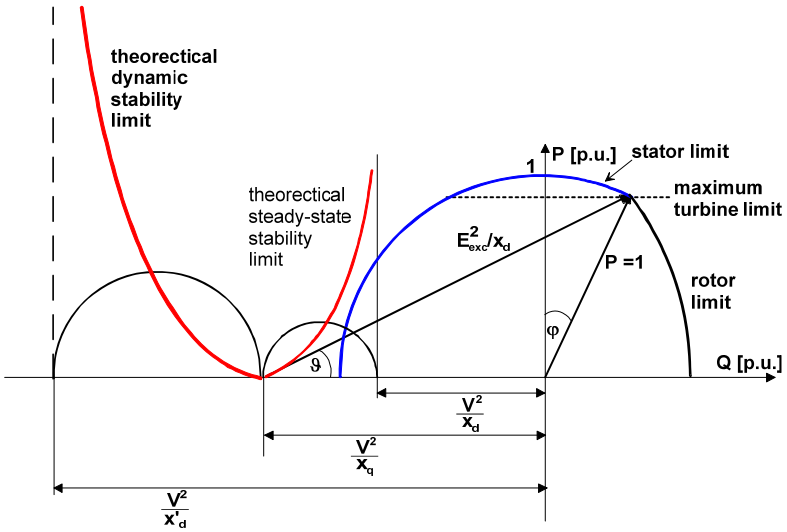

Figure 6: Dynamic stability limit (salient pole generator)

In figure 7 the statements regarding the limits during loss of filed (under-excitation) are summarized. They are:

- The practical (steady state) stability limit is to the right of the theoretical value and is given by the capability diagram of the generator. It applies at nominal voltage.
- If the generator is operated with a voltage $V < V_N$, the limit is shifted to the right.
- To consider „dynamic conditions“, a dynamic stability limit is introduced. If it is exceeded, the machine must be disconnected from the system immediately, as a pole slip will most likely take place.

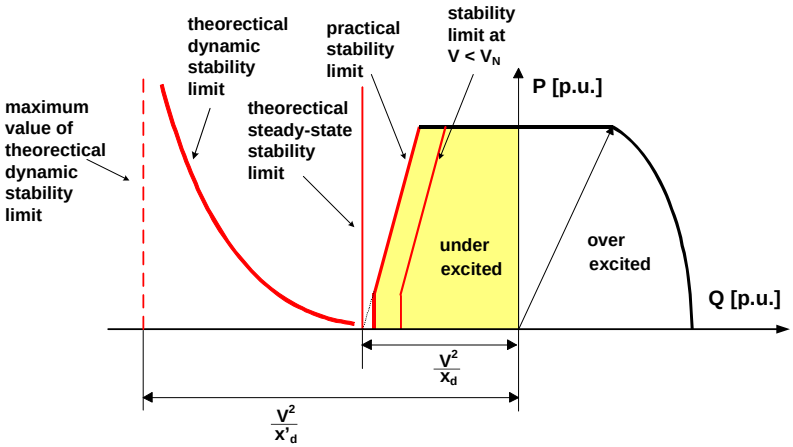

Figure 7: Summary of the statements regarding stability limits

For both generator types - salient pole and turbo generator - the stability limits (steady-state and dynamic) are calculated in an example by using equation 1 and 2.
The following data are used:

Salient pole generator:

Generator terminal voltage V =1.0;
Rotor voltage E = in steps (0; 0.25; 0.5; 0.75; 1.0; 1.68)
Reactances: $x_d = 1.0$; $x_q = 0.6$; $x_d' = 0.3$;

Figure 8 shows the calculation results. The “half” circles represent the P= f (Q) for different angles (from 0° to 180°) and the selected rotor voltage E. The stability is reached at the maximum of the active power (dP/dϑ = 0). The practical steady-state stability is calculated with a safety margin of 9 %. For the dynamic stability limit the same calculation was done with the transient direct axis reactance.

Turbo generator:

Generator terminal voltage V =1.0;
Rotor voltage E = in steps (0; 0.4; 0.8; 1; 1.5; 2.51)
Reactances: x_d = 1.919; x_q = 1.885 x_d' = 0.35;

Figure 9 shows the calculation results for turbo generator.

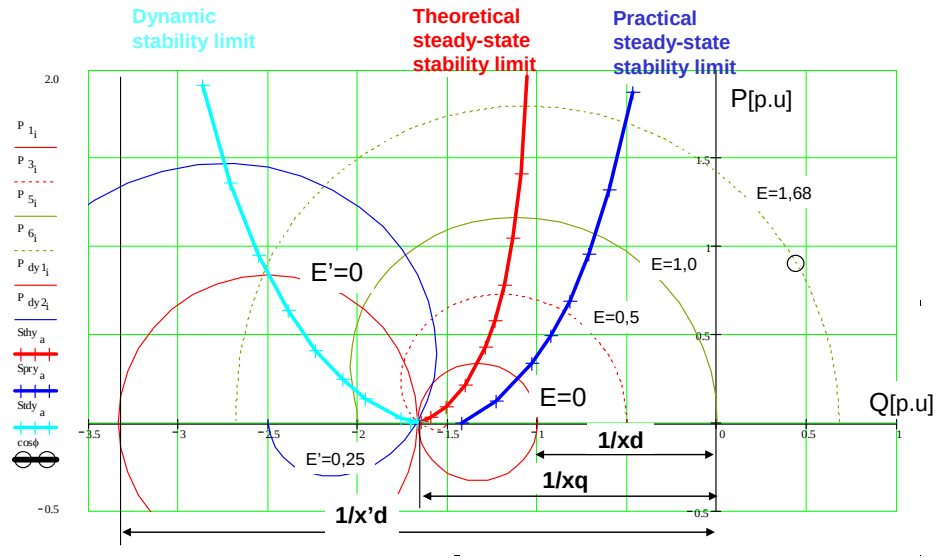

Figure 8: Calculated stability limit of a salient pole generator.

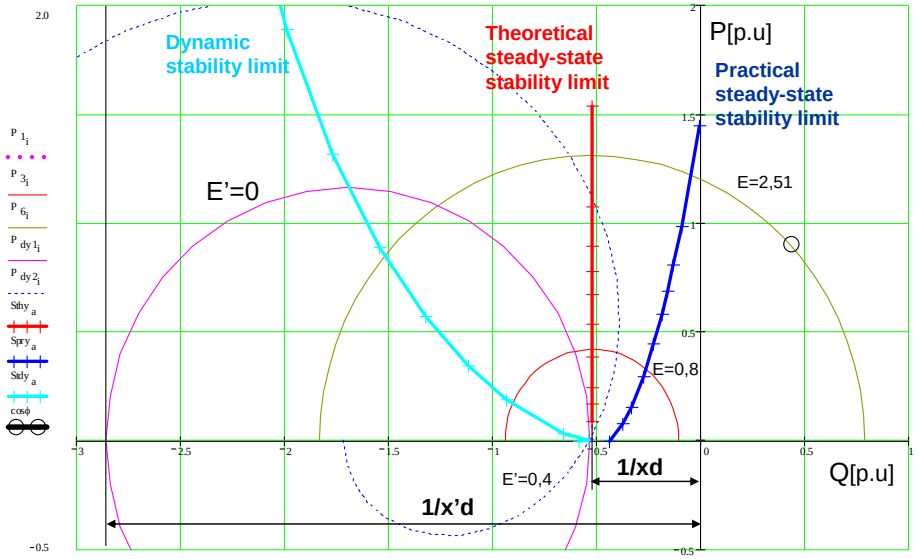

Figure 9: Calculated stability limit of a turbo generator.

The loss of synchronism by a salient pole generator is illustrated in figure 10 [3]. In the diagram the increase of the rotor angle following loss of excitation can be seen. Due to the constant turbine power, the real power does not change, the imported reactive power increases and the steady state stability

limit is exceeded. As a result of the slip an additional flux appears in the excitation circuit or an additional induced rotor voltage appears which attempts to maintain the armature reaction of the machine at a constant level. This is apparent from figure 10 where in the range between 90° and 180° the excitation current increases significantly again. Only shortly before 180° is the rotor accelerated towards the stator pole (zero load state with inverted pole). This large acceleration causes large slip and thus increased influence by the damper windings. When ϑ = 180° the flux change and therefore the (no longer measurable) rotor voltage becomes equal to zero. As this takes place in an inductive circuit, the zero crossing of the excitation current and the measured rotor voltage is delayed. The rotor is now decelerated until it almost reaches synchronous speed as the synchronising torque shortly after ϑ = 180° becomes very large. The result of this is a high torque impulse that is also noticeable as a significant real power impulse (refer to Figure 10a). The mechanical power driving the machine is however too large to allow a recovery and the machine will continue slipping. Between ϑ = 180° and 360° and also between n 180° and (n+1) 180° this sequence is repeated. Some deviations apply during the transient state before the steady state slip condition is reached. The reactive power minimum following the first torque impulse therefore has a different value compared to the following swing cycles. The swing and transient conditions are particularly severe in the salient pole machine due to the difference in direct axis and quadrature axis reactance. The slip changes dramatically during one cycle.

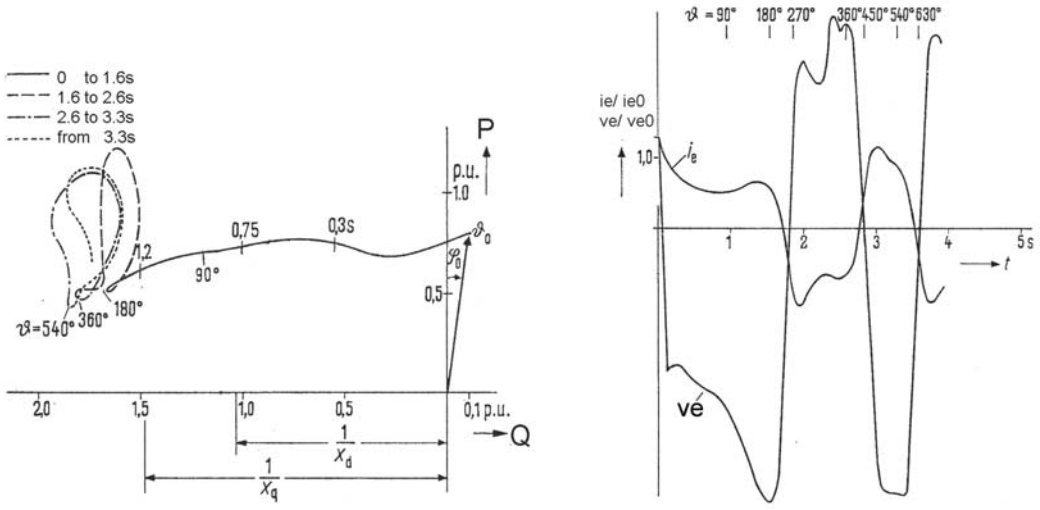

a) b)

Figure 10: Loss of synchronism condition on a 30-MVA-salient pole generator (caused by rapid loss of excitation) with P= 0.8, ie =1.3*ie0 [3]
[a) course of power flow; b) excitation signals (ie =excitation current, ie0= zero load nominal excitation current, ve = excitation voltage, ve0 = zero load excitation nominal voltage]

3. Admittance measuring principle

As mentioned in the introduction, the transformation of the capability diagram into the admittance plane has the distinct advantage that when using the p.u. representation, a direct reference to the generator capability diagram is provided, that is independent of the actual generator voltage.

The transformation is explained by the following equation:
The equations (5) and (6) describe the fundamental definition of the complex power and the complex admittance.

$$\underline{S} = \underline{V} * \underline{I}^{*} \qquad \underline{S} = P + jQ \qquad (5)$$

$$\underline{Y} = \frac{\underline{I}}{\underline{V}} \qquad \underline{Y} = G + jB \qquad (6)$$

with: Y admittance
G conductance (real component of the admittance)
B Susceptance (reactive component of the admittance)

The relationship for the transformation can be derived by multiplying in equation (6) with the conjugated complex voltage.

$$\underline{Y} = \frac{\underline{I} \cdot \underline{V}^*}{\underline{V} \cdot \underline{V}^*} = \frac{\underline{S}^*}{V^2} = \frac{P - jQ}{V^2} = \frac{P}{V^2} - j\frac{Q}{V^2} \qquad (7)$$

Comparing the coefficient in equation (6) and (7) it results in the definition of the admittance values.

$$G = \frac{P}{V^2} \qquad B = -\frac{Q}{V^2} \qquad (8)$$

The values from the axis in the generator capability diagram must simply be divided by the square of the voltage. If subsequently the sign of the reactive component is inverted, the transformation is complete. When $V = V_N = 1$, the per unit numerical values in the capability diagram are identical with those in the admittance diagram (refer to figure 11). From the per unit capability diagram it is therefore possible to directly derive the setting values of the loss of field protection.

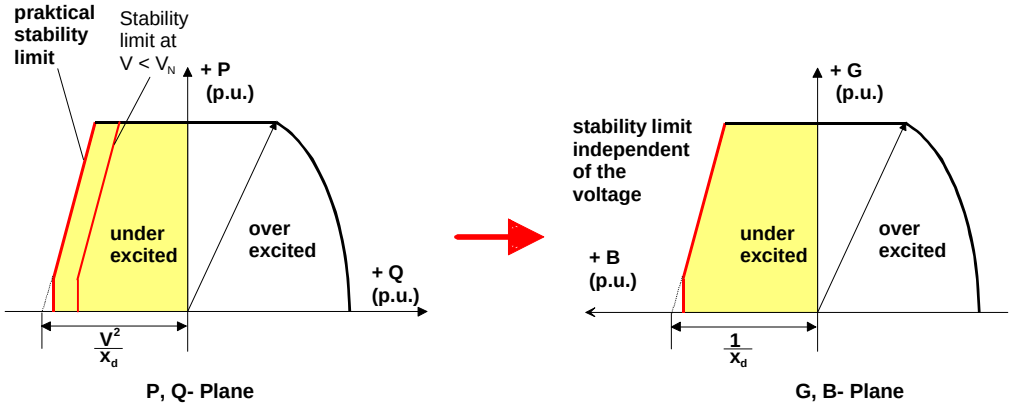

Figure 11: Capability diagram of the generator and admittance diagram

The protection measuring algorithms are based on the equations (5) and (8). The vector signals are derived from the sampled instantaneous values in the 3 phase to ground voltages and the 3 phase currents. The positive sequence components are calculated from these vectors. According to the definition in equation (5), the positive sequence voltage and current components are employed to calculate the active and reactive power. Division by the positive sequence voltage V1 according to equation (8), results in the transformation from the power plane into the admittance plane. To avoid over functions in the case short circuits close to the generator terminals an undervoltage blocking is implemented. The threshold is fixed at V1 = 25 % of the nominal voltage.

Figure 7 can be used to extract the characteristics required by the protection functions. The given static stability limit must be monitored. Generally 2 lines are sufficient for this purpose. An additional threshold value which depends on the dynamic stability limit applies. From the area of extreme underexcitation (on left of char. 3), it is highly unlikely that the machine will recover to the stable operating range. Fast tripping is therefore required in this case. This is different if the static stability limit is exceeded (char. 1 and 2 in figure 12). In this case, if the excitation voltage is still sufficiently large, a recovery by the machine to the stable operating range is not inconceivable. The monitoring of the excitation voltage (V_{exc} <) is therefore introduced as an additional criterion. This criterion controls the tripping time of char. 1 and 2. In this way, over functions as result of transient transgression of the static stability limit due to dynamic impulses that are followed by a recovery to statically stable conditions, are prevented.

To set these characteristics, the setting parameters that consist of the intersection with the B-axis as base point of the line, and the inclination, are applied. The angle of inclination may be derived from the generator capability diagram (refer also to section 5). The setting should be such that it is close to the given stability characteristic. The excitation circuit controller characteristic supersedes this.

The setting threshold of excitation voltage supervision is approximately 50% of the no-load excitation voltage (V_{exc0}).

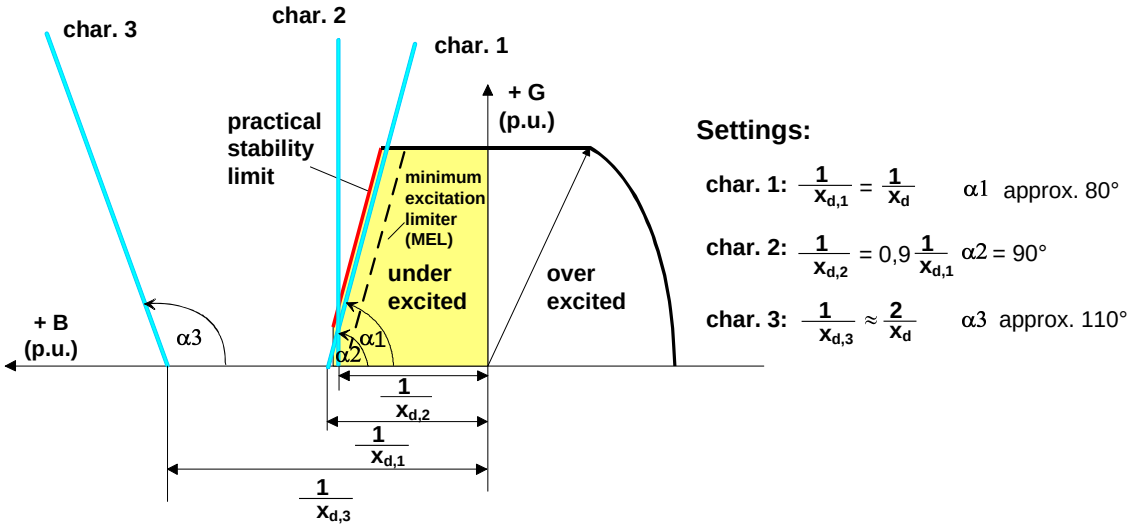

Figure 12: Characteristic of the admittance protection (turbo generator) [8]
(At salient pole generators char.1 is approximately $1/x_d$ +1/2($1/x_q$ -$1/x_d$) and char.2 is approximately $1/x_d$ with $\alpha 2 = 100°$)

The protection response resulting from the characteristics in figure 12 is the following. To avoid over functions by the loss of field protection due to transient phenomena (e.g. out of step conditions) a time delay is recommend.

a) *characteristic 1, 2 exceeded, excitation voltage monitoring (Vexc <) not picked up*
This condition must be alarmed, and when configured, tripping with long time delay (approx. after 10 s) is carried out.

b) *characteristic 1, 2 exceeded, excitation voltage monitoring (Vexc <) picked up*
For this condition, tripping with short time delay (approx. **0.5 s** to 1.5s) is required.

c) *characteristic 3 exceeded*
For this condition, tripping with short (0.3 s), or no time delay (after transient studies) is required.

Figure 12 shows additional the characteristic of the minimum excitation limiter (MEL), which is a control function. The MEL acts to limit the reactive power (Var) flow into the generator. When the reactive power flow into the generator excesses the MEL setpoint, the MEL becomes active to increase terminal voltage which reduces the reactive power in-flow. The voltage increase continues until the reactive power flow is reduced below the MEL setting [9]. The loss of field protection must be coordinated with the MEL. The MEL realization should also consider the voltage behavior due to a reduced terminal voltage (see figure 7).

4. Comparison with the impedance measuring

As stated in the introduction, the impedance measuring principle is widely applied [1, 2]. To obtain the setting parameters for the impedance principle, the generator capability diagram must be transformed (mapped) into the impedance plane. This transformation mathematically corresponds to the mathematical inversion of a locus. Consequently, the direct reference to the capability diagram is lost. In accordance with the locus theory, (a line that just misses the origin becomes when inverted a circle that touches the origin), the transformation of the theoretical stability characteristic to the impedance plane results in the section of a circle. This transformation is illustrated in Figure 13. All points to the left of the stability limit in the capability diagram are located inside the semi-circle (shaded area) in the impedance plane.

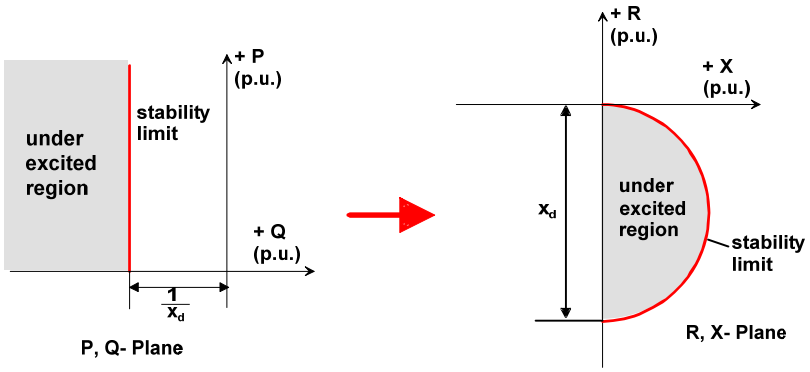

Figure 13: Transformation in the impedance plane

Conversely, the characteristics in accordance with IEEE [1] can be converted to the per unit generator capability diagram. The following rule must be observed here: circles which do not pass through the origin, will again give circles when inverted. Figure 14 shows the transformation. It is apparent that in comparison to the admittance principle (refer to figure 12) this provides a much rougher approximation of the stability characteristic. This measuring principle cannot detect if the stability limit provided by the generator manufacturer is continuously exceeded by a small amount. The control system (MEL) or the operating personnel must be relied upon to detect such failures. Alternatively, additional monitoring (e.g. additional impedance circle) must be provided.

The greater margin is however of advantage during dynamic situations (transient transgression of the stability characteristic). Such incidences do not result in pick up, or only result in transient pick up, by the protection. Additionally, the significant points, as well as the rules for the transformation are indicated in figure 14.

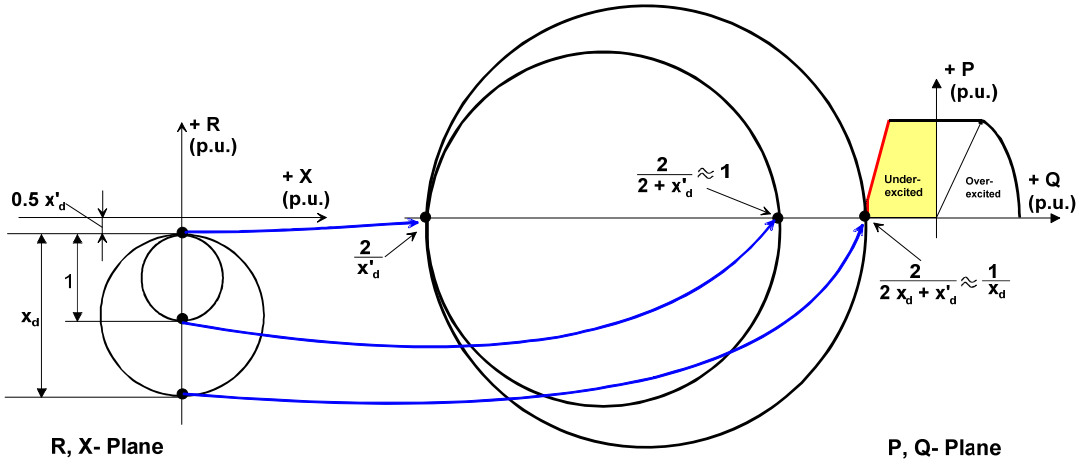

Figure 14: Transformation of the IEEE –impedance characteristic to the capability diagram

In figure 15 a summarized comparison of the admittance and impedance measuring principle is shown for a turbo generator. The typical setting recommendations were considered for this purpose (refer to figures 12 and 14). For example, in the case of under-excitation, the admittance measurement can, as a result of it's more accurate match to the static stability characteristic, provide an early alarm. This may be seen from the indicated trajectory in the event of under-excitation. Furthermore figure 15 shows that the two measuring techniques are largely similar. The significant differences may be found in the thresholds.

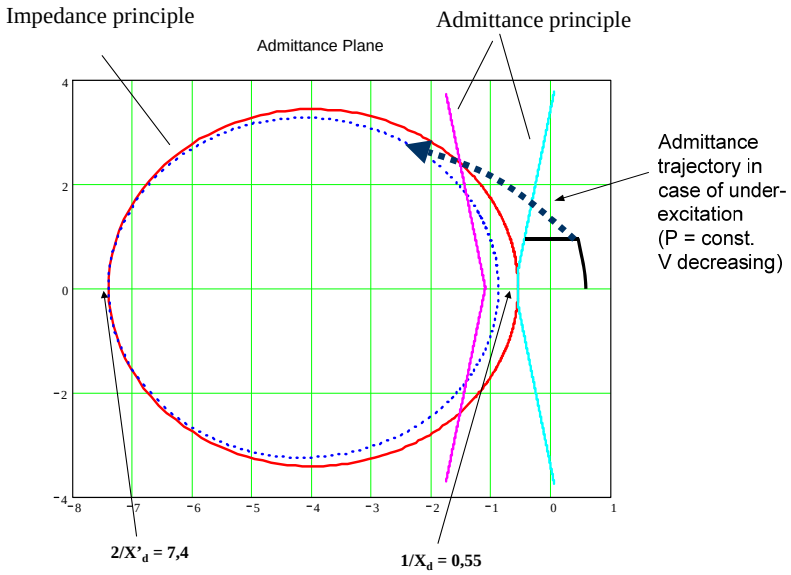

Figure 15: Comparison of the impedance and admittance measurement loci in per unit – capability diagram (x_d = 1.81; x'_d = 0.27)

5. Application

In this section, the following question is addressed: how are the setting values derived?

The question is essentially answered in sections 2 to 4. Depending on the available information, the different methods for obtaining the setting parameters are employed:

a) If the generator capability diagram is available, the setting parameters may be derived directly there from (per unit representation required). Settings for characteristic 3 are derived according to figure 12.

b) If the direct axis reactance of the generator is known, the setting values may be directly obtained from the recommendations given in figure 12. For the slopes, the indicated angles must be used. This recommendation is in accordance with the IEEE recommendation. [1].

c) If the protection is replaced in the course of a protection refurbishment, the previously used impedance settings can naturally be converted to admittance settings. Assuming secondary setting values, the following equation provides the conversion to secondary per unit admittance values.

$$\frac{1}{x_{d,sec}} = \frac{V_{N,Sec}}{\sqrt{3}\, I_{N,Sec} \cdot X_{old,Setting}} \qquad (9)$$

with:
$V_{N,Sec}$ secondary nominal voltage (e.g. 120V)
$I_{N,Sec}$ secondary nominal current (e.g. 5A)
$X_{old,Setting}$ „old“ previous setting in Ohm

In figure 16 a practical example of the parameter conversion is shown. The left hand section of the diagram indicates the previous characteristic and possible setting values of the protection that is to be replaced. The right hand section shows the setting table of the numerical protection with the converted parameters. With the conversion equation (9), the reactances are converted to per unit values. Furthermore, the excitation voltage monitoring is not used. The three characteristics of Figure 12 are therefore applied separately. Characteristic 1 is used for alarm purposes. With the angle of 80°, a good estimate of the stability limit is achieved. The time delay for the alarm was set to 10 s. Additional an alarm signal is automatically generated if the admittance is over the characteristics (OR logic) and stored in the puffer named “trip log”. Characteristic 2 provides the replica of the larger impedance circle of the previous protection and trips with short time delay. The converted susceptance value for

characteristic 2 is 0.51 and a time delay of 1 s was selected. To achieve a better match to the circle, the characteristic is slightly tilted to the left (refer to figure 15), and a setting of 100° was chosen.

With these setting parameters, characteristic 3 corresponds to the inner circle.

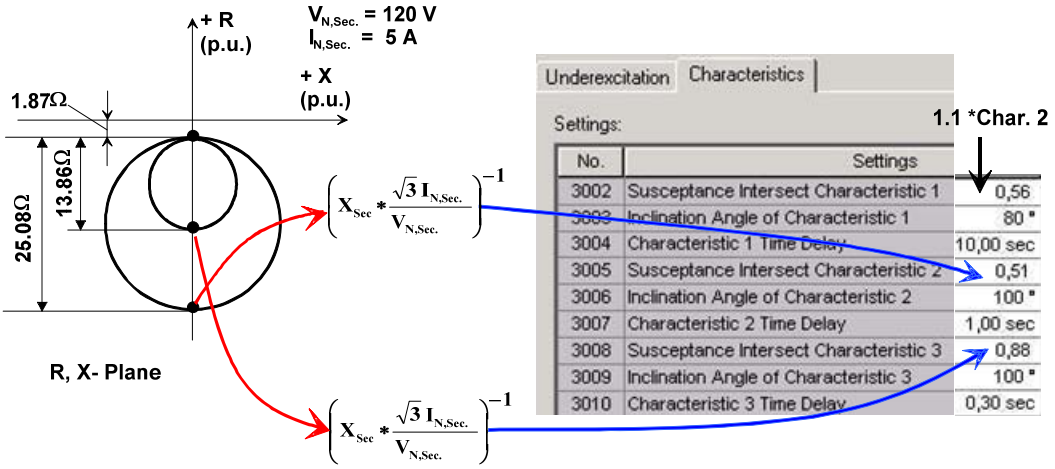

Figure 16: Conversion example: impedance to admittance values

6. Testing of the characteristic

The main objective of the test is the verification of the settings. As the characteristics are made up of straight lines, two test points result: the base point (BP) of the lines (I) and a further point on the line (II). The test is carried out with the nominal voltage. As test variable, the current is changed in amplitude and phase.

During the test to establish the base point, the current leads the voltage by 90° (capacitive current). The value of the current is derived by multiplying the set value with the nominal secondary current (example: Char. 1: 0.56 * 5 A = 2.8 A). The injected test current is therefore 2.8 A with a phase angle of + 90°.

The test of the second point (II) is preferably carried out at an angle of + 45°. The injected test current is derived from the intersection of the tested characteristic with the line along which is tested. The test current is calculated by defining the equation of the two lines, and equating the intersection. Alternatively, the intersection can be derived graphically. Figure 16 shows the results in a graphic. The line equations for computation of the intersection are also shown. On the right side of the figure the test voltage and current are shown for the two test points (I, II). Drawn is only one phase of the three phase system. The current is leading (capacitive). For testing the behaviour during an undervoltage situation (shift of the characteristic to right (see figure 7)) the test voltage and current must be reduced by the same ratio. Shall be the test done with 90% of the rated voltage, than the voltage and current for the 100% case must be multiplied by the factor 0.9 (e.g. test point (I): V = 0.9 * 120V/√3 = 108V/√3 and I = 0.9 * 2.8 A = 2.52 A).

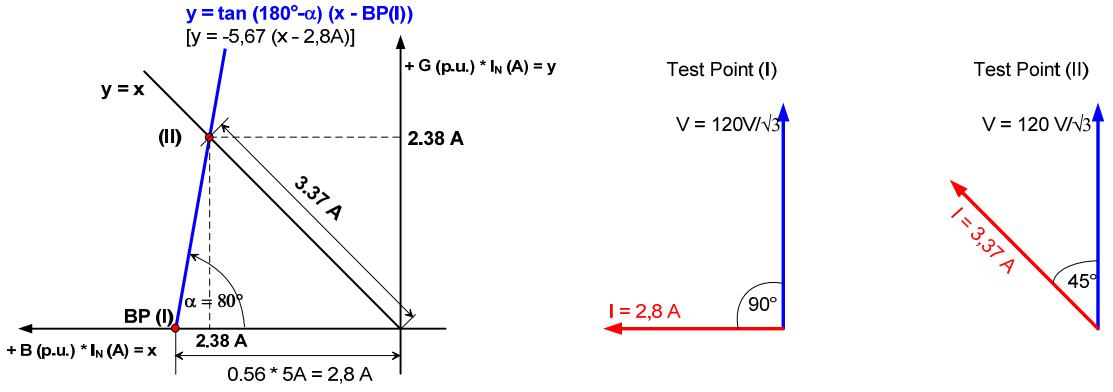

Figure 17: Testing of the loss of field characteristic

7. Transient behavior of loss of field protection

The transient behavior of the protection can only be shown with real failures or with dynamic simulations. For dynamic simulation two methods are used:

- **Real time digital simulator (RTDS)**
  The generator and a network is simulated. All numerical calculations are done in real time. Via amplifiers the transient data can be injected into the relay directly. Closed loop test are possible.

- **Transient network calculations program**
  The generator and a network is simulated. The transient calculations are done offline. The result of the simulation can be stored in a comtrade file. With this file the protection function can be test via digital test equipment. In this case only an open loop test is possible.

A 200 MVA generator with a step-up transformer and network was simulated with a RTDS system. The protection measures the phase current from the star point side and the phase to ground voltage from the terminal of the generator. A loss of field situation was initiated by a voltage regulator failure (voltage jump from V = 1.08 to 0.8). The generator operated under full load condition (P = 160 MW, Q = 25 MVar; field current if = 1.87 If0). The loss of field protection tripped with characteristic 3, because for the characteristic 1 and 2 a time delay of 10 s was set. Figure 18 shows the stored fault record from the device. To get a better overview only one phase (B = L2) plus the important binary traces are drawn. A reduction in the voltage and increased phase current can be seen. The binary traces show the pickup (trajectory is over char. 1) and the trip via char. 3 (Exc<3 TRIP). In addition figure 19 shows the calculated admittance and the used characteristic 1 and 3. The time between the crosses is 50ms. The longer distance indicates an increasing of the slip, which can be clear seen if the trajectory crosses char. 3 (left straight line).

To get from the users practical loss of field failures is very seldom. Figure 20 shows such a record and the analysis with the graphic tool SIGRA. During the commissioning of a pump storage station it was not possible to open the generator circuit breaker. The generator was in the pump mode (motor operation). By the operator the field breaker was opened. On the left side of the figure the phase voltage and current is shown in RMS values. Below are the binary traces. The pickup and the trip event are recorded. The event “Exc<U< Trip” means that the trajectory is over characteristic 1 and additional the field voltage supervision (V_{exc}<) picked up. The time delay was set 1 sec. The loss of excitation voltage can be seen by trace TD3. The right side of the figure shows the calculated impedance and power. The cross in the P, Q plane marks the trip by loss of field protection. While the generator CB was out of service the breaker failure protection becomes active and tripped the high voltage CB after a delay of 0.5 sec. The open high voltage CB can be seen by the interrupted phase current.

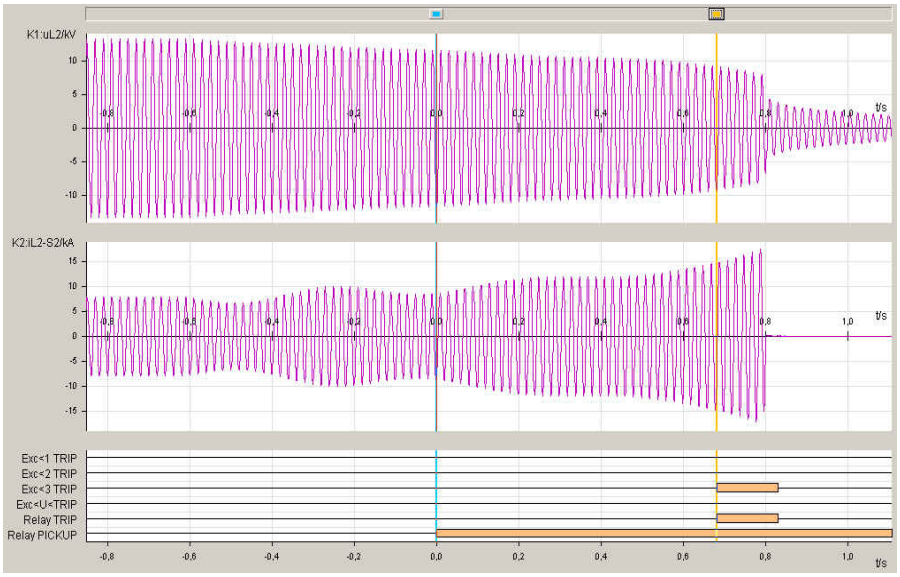

Figure 18: Transient test with RTDS (char 1: 0.55∠80° 10s; char 2: 0.51∠90° 10s; char. 1.1∠110° 0s)

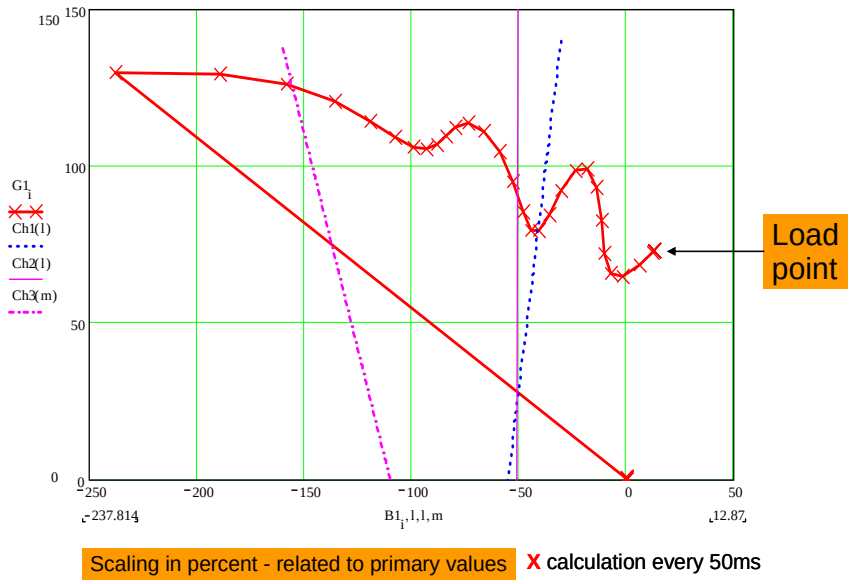

Figure 19: Calculated admittances

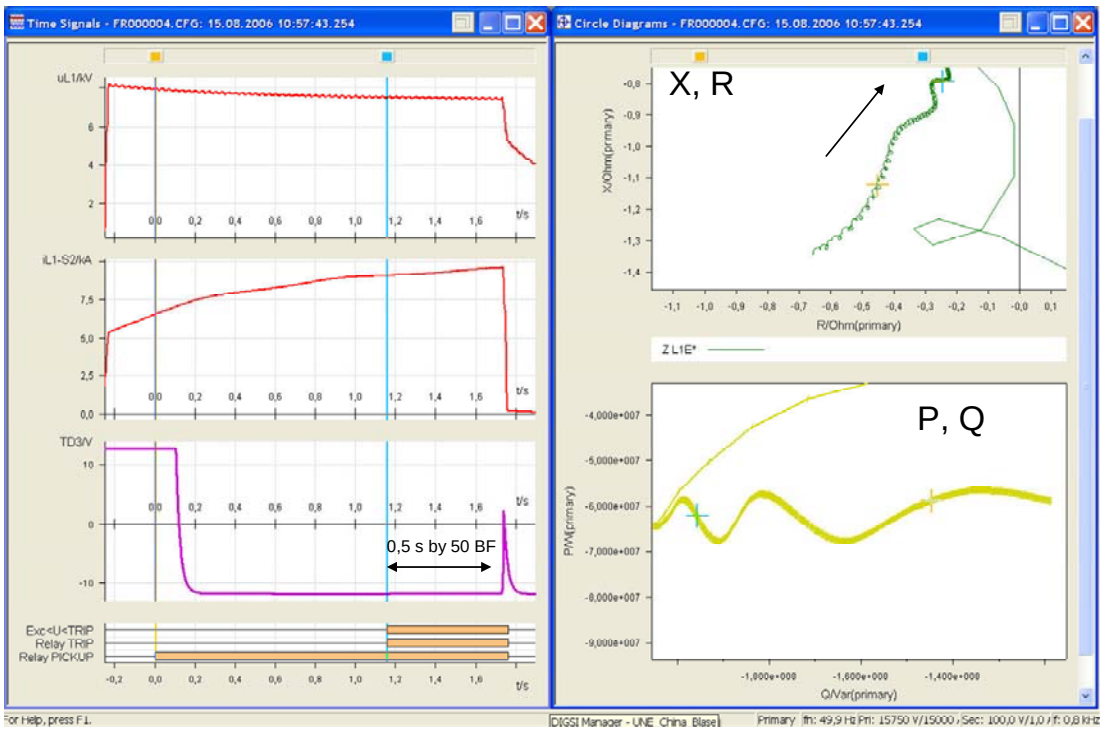

Figure 20: Trajectory during a real loss of field failure.

8. Summary

The static stability limit is given by the generator capability diagram. This limit is closely matched by the admittance measurement. It correctly takes into consideration the influence of the generator voltage on the capability diagram.

The loss of field of both basic generator types, salient pole and turbo generator, was explained at length. The fundamentals of the stability limit and the signals that influence it were discussed. Subse-

quently the transformation from the capability diagram to the admittance plane, admittance measuring technique and implementation of the under-excitation protection function, was looked at. Furthermore the differences relative to the impedance measurement and the transformation of the capability diagram to the impedance plane were dealt with. The section “Applications” was dedicated to the calculation of the setting values and showed the different solutions. The scope of testing is reduced to a minimum by employing numerical technology. A method for the verification of characteristic setting values was shown. Additionally the transient performance of the loss field protection was briefly demonstrated with two examples.

Literature:

[1] IEEE Guide for AC Generator Protection. IEEE Std. C37.102 – 1995, Approved 12 December 1995, ISBN 1-55937-711-9

[2] IEEE Tutorial on the Protection of Synchronous Generators. (1995) IEEE Catalogue Number: 95 TP 102

[3] Fischer, A., Zurowski, E: „Neuartiger Untererregungsschutz“ (New type of under-excitation protection*)Siemens magazine , (1966) paper.8, p. 634 – 640

[4] Untererregungsschutz (under-excitation protection*) RG66, product pamphlet of Siemens, 1967

[5] Bonfert,K : Betriebsverhalten der Synchronmaschine (synchronous machine operational response*). Berlin, Göttingen, Heidelberg, Springer-Verlag 1962

[6] Weßnigk, K.-D.: Kraftwerkselektrotechnik (power station electronics*). vde verlag gmbh, Berlin, Offenbach 1993, ISBN 3-8007-1724-7

[7] Born,E.; Fischer, A.:Elektronischer Untererregungsschutz (electronic under-excitation protection*). Siemens-magazine. (1972) paper.12; p. 912 –915

[8] Multifunction Generator, Motor and Transformer Protection Relay 7UM62. (2008) Siemens Manual, order No. C53000-G1176-C149-6

[9] Reimert, D.: Protective Relaying for Power Generation Systems. Taylor @Francis, ISBN 0-8247-0700-1, 2006

* these titles only available in German.